2021

Raising the bar during early immunotherapy for cancer: simple mathematical models may help distinguish temporary vs. ultimate progression

Charles F. Babbs

Raising the bar during early immunotherapy for cancer: simple mathematical models may help distinguish temporary vs. ultimate progression

Charles F. Babbs, MD, PhD, Weldon School of Biomedical Engineering, Purdue University, West Lafayette, Indiana, USA Email: babbs@purdue.edu

ABSTRACT

Background: The apparent success of immunotherapy depends on the duration of follow up, sometimes with little evidence of efficacy during the first 4 to 8 months and often some degree of "pseudoprogression". Differentiating transient pseudoprogression from true progression that would require a change in therapy can be challenging. The present study uses mathematical modeling and simulation to account for the unique kinetics and delayed clinical effects of immunotherapy and suggests improved approaches to predict efficacy and patient response from imaging studies.

Methods: A mathematical model of tumor cell-immunocyte interaction is exercised to simulate a large number of individual patients and to derive surrogate endpoints for success or failure from the ratio of tumor diameter at 2, 4, 6, 8, 10, or 12 months follow up to initial tumor diameter. The simplified predator-prey model includes 4 lumped parameters: net tumor growth rate, g; immune cell killing efficiency, k; immune cell signaling, λ; and immune cell half-life decay, μ. Differential equations, $dT/dt = gT - kL$ and $dL/dt = \lambda LT - \mu L$, for numbers of tumor cells, T, (the prey) and immunocytes, L, (the predators) are solved numerically as functions of time, t , with ranges of g, k, λ, and initial conditions estimated from clinically available data. Tumor diameters, d, are proportional to the cube root of T + L. Apparent progression is defined when the time-varying diameter ratio, d/d_0, exceeds a pre-defined, adjustable threshold. True progression is defined as $d/d_0 > 1$ at 24 months follow up or $T/T_0 > 10$ at any time.

Results: Depending on initial conditions, the model equations predict either simple or complex dynamics, including cyclic increases in tumor cell numbers prior to a population crash to zero, apparent cure with late recurrence, and better long-term outcome with initially smaller lymphocyte numbers. Simulations of 4000 such complex cases show that $d/d_0 > 1.0$ at 2 to 6 months is a poor predictor of true progression, and often signals pseudoprogression. However, raising the bar or threshold for defining progressive disease from $d/d_0 > 1.0$ to $d/d_0 > 2.0$ during the first 6 months of immunotherapy and lowering the bar to $d/d_0 > 0.5$ after 6 months can eliminate most instances of pseudoprogression and lead to better over-all outcomes.

Conclusions: Mathematical models can account for the complex dynamics of immune-tumor cell interactions that make accurate clinical decisions to continue or discontinue treatment difficult. The present model and approach can be adapted and calibrated to data for different types and stages of cancer and help to optimize treatment success.

Keywords: agent-based model, checkpoint inhibitors, classifier, cutoff, delayed response, immune modulation, iRECIST guidelines, kinetics, optimization, predator-prey, pseudoprogression, response criteria, T-cell response, tumor infiltrating lymphocytes

INTRODUCTION

Kinetics of conventional chemotherapy for cancer are fundamentally different from those of immunotherapy(3, 33, 42). In conventional chemotherapy cell kill happens initially and rapidly, until most susceptible cells are killed or toxic side effects supervene. Toxicity to normal tissues is severe and dose related, and the maximal therapeutic effect happens very near the maximum tolerated dose. Both therapeutic and toxic effects are related to tissue and blood concentrations of the drug, as described by classical pharmacokinetics. These features are very much different from those of immunotherapy for cancer, as summarized, for example, by Hoos(21).

In immunotherapy treatment effect is not proportional to toxicity, dose, schedule, or blood levels of drug. The optimal biologic dose is often not the maximum tolerated dose. Cell kill grows exponentially with time, as immunocyte numbers grow, beginning at a low level and ultimately reaching a crescendo with a sudden crash in tumor cell numbers. Early tumor shrinkage is not a consistent predictor of survival. Instead, clinical benefits can be delayed and can occur after an apparent increase in tumor tissue volume, which would be classically characterized as progression, and which would likely lead to discontinuation or to change in approach before any benefits are realized. This initial surge in tumor burden, followed by tumor shrinkage, has been termed “pseudoprogression”(7, 33).

Such differences in kinetics and toxicity require a new therapeutic mindset in evaluating whether a treatment is working(3), as well as a new conceptual approach to clinical trial design(18, 22). In particular, determining the end point of successful therapy may require more patience, more tolerance of modest early tumor growth, and more time for observation to determine if the immunotherapy is actually working. Such tolerance of continued tumor growth is concerning for physicians and patients accustomed to ordinary chemotherapy. Better knowledge of the kinetics of immunotherapy can help both physicians and patients understand the delayed nature of tumor necrosis in a course of immunotherapy and avoid the temptation to quit too soon.

Accordingly, there is a need for new guidelines to distinguish temporary progression from ultimate progression in immunotherapy of cancer, both in clinical trials and in daily clinical practice. Already, the virtues of such innovative guidelines have been discussed(36) in terms of “raising the bar” for the definition of progressive disease in trials of immunotherapy in order to better identify patients with previously unrecognized benefit, despite delayed responses. Although cancer biology and immune system biology are exceedingly complex(4), in some cases simplifying such a problem in an abstract way can make it easier to solve. At zero risk to patients and essentially zero cost, mathematical models can describe cell kinetics in a rigorous, quantitative way(15, 24). By focusing on crucial factors and deliberately disregarding secondary effects, a mathematical models can provide useful descriptions of a complex biological processes. Accordingly, the goal of the present study is to examine results of mathematical simulations of immunotherapy for cancer in large numbers of different patients to identify improved predictors of ultimate outcome, despite pseudoprogression.

METHODS

Previously, ordinary differential equation models similar to those used in ecology(6) and epidemiology, in which cells are considered as individuals in interacting populations, have led to important insights for cancer research and clinical practice(2, 15, 19, 25, 26). The present paper describes mathematical modeling of the time histories of tumor growth and shrinkage during immunotherapy to identify patterns during the first 12 months of follow up that distinguish effective from futile therapy. The research methods include the following steps.

1. Implement a previously published and simplified kinetic model of immunotherapy

2. Develop a Monte Carlo technique for simulation of a large series of clinical cases, in which imaging data for each case during the early months of follow up are correlated with ultimate outcome at two years

3. Specify typical values of model parameters that can be modified, based on clinical knowledge and data, for different cancer types and stages

4. Define appropriate ranges of model parameters and statistical sampling methods

5. Calculate time histories of tumor growth at 2, 4, 6, 8, 10, and 12 months follow up for many individual patient simulations

6. Construct histograms of diameter ratios at each follow up time for cases of either ultimate success or ultimate failure (true progression) at 24 months

7. Test possible time-varying “raised bars” for the definition of apparent progression and determine their effect on the prediction of ultimate progression.

Part 1. Kinetic model of immunotherapy

As previously described in detail(3) one can represent mathematically the predator-prey dynamics of immunotherapy for a population of growing tumor cells (the prey) that are killed upon contact with cytotoxic immune cells (the predators). Each population is considered to function collectively. Although the actual populations of tumor and immune cells have diverse players with distinct capabilities; at the population level, the outcome of the contest between predators and prey can be represented in terms of the balance of power between [prey population size × average growth rate] versus [predator population size × average killing effectiveness].

Let T denote the number of tumor cells and L denote the number of immune cells (lymphocytes and activated macrophages). The rate of change in tumor cell numbers (dT/dt) as a function of time, t , is increased by the net growth rate and decreased by immune mediated cell killing. The rate of change in immune cells (dL/dt) is increased by lumped tumor-lymphocyte interactions and signaling, and decreased by spontaneous lymphocyte death. Two equations describe the overall population cytokinetics:

$$\frac{dT}{dt} = gT - kL \qquad (1)$$

and

$$\frac{dL}{dt} = \lambda TL - \mu L \, . \qquad (2)$$

Constant, g , represents net tumor cell growth minus non-immune mediated cell death. Constant, k, represents the average killing effectiveness of all immune cells in the predator "army". Constant, λ , represents positive feedback of cell-cell signaling on lymphocyte recruiting, for example from release of tumor antigens or from release of cytokines by active lymphocytes. Constant, μ , represents spontaneous death and emigration of immune cells. Equation (1) describes the net replication rate in absence of tumor immunity, minus the rate of killing by immunocytes. Equation (2) describes the recruitment of immune cells from cell-cell signaling, minus the spontaneous death of immune cells. As pointed out by Agur(2) the underlying kinetics depend on three major factors: the size of the tumor cell population, T, the size of immune cell population, L, and the strength of the interactions between the two populations, k and λ. The lumped interaction term, λ, includes multiple effects in aggregate, for example changes expression of histocompatibility complex antigens by tumor cells, which may weaken their detection by cytotoxic lymphocytes, as well as the physical ability of immune cells to penetrate the tumor, as in the case of the blood brain barrier in admitting only activated lymphocytes or preferentially admitting immunosuppressive Treg type lymphocytes(26).

Initial conditions describe the state of the tumor at the time of diagnosis. T_0 is the size of the initial pre-treatment tumor cell population, and $T(t)/T_0$ represents the fraction of the initial tumor cell mass remaining at time, t , after treatment is begun. To specify initial conditions, the number of lymphocytes is also normalized by the initial number of tumor cells, so that L_0/T_0 represents the initial immune cell population within the tumor.

Examination of limiting cases helps to clarify how the model works. When t = 0, then $T = T_0$. When k = 0 (no tumor cell killing), dT/dt = gT, dT/T = gdt, and by integration, $T = T_0 e^{gt}$ with unopposed tumor growth. When $\lambda = 0$ there is initial tumor cell killing by the original L_0 lymphocytes, but no recruiting of additional immune cells. In this case, the immunocytes decay exponentially so that $L = L_0 e^{-\mu t}$, and in turn, $dT/dt = gT - kL_0 e^{-\mu t}$, with only a transient dip in tumor cell growth.

An interesting and useful special case is that of an unstable steady-state, in which the tumor neither grows nor shrinks in size. This condition represents a stalemate with zero net growth in either the immune cell population or the tumor population. Then $\frac{dT/T_0}{dt} = 0 = g - k\frac{L_0}{T_0}$, so that $k = gT_0/L_0$. Also, at stalemate $\frac{dL}{dt} = \lambda L_0 T_0 - \mu L_0 = 0$, so that $\lambda T_0 = \mu$. These relationships help to simplify estimation of model parameters from clinically available data, as shown in Part 3 below for a generic solid tumor model. To model histories of tumor growth or shrinkage, Equations (1) and (2) are integrated numerically using the simple Euler method, implemented, for example, in Visual Basic code within an Excel spreadsheet, using a sufficiently small value of Δt , such as 0.001 day, a typical run time on a laptop computer being 0.3 sec per individual patient.

Part 2. Monte Carlo technique for simulation of a clinical trial

By accumulating a very large number of simulated cases using Equations (1) and (2) with different parameter sets, one can use Monte Carlo simulations as a flight simulator for testing classification rules. The values of the various model parameters in each case are selected from probability distributions representing ranges of values expected in a particular patient population, including both failed and successful treatments. Here, for any one simulation, a sample is selected from a uniform random distribution ranging from a chosen lower limit to a chosen upper limit for each parameter g, k, λ, mu, and T_0/L_0. Specification of these limits is explained in Part 4. A sample of 4000 simulated cases was sorted into classes representing "success" and "failure" or ultimate progression. The definition of success was ($T/T_0 < 1$ and $dT/dt <= 0$), representing either tumor elimination, continuing tumor shrinkage, or durable stable disease at 24-month follow up. For clinical realism, success also required that T/T_0 not exceed 10 at any time during the simulation. This limit is in lieu of the "carrying capacity" constant, K, of Agur(26). Any result other than success is interpreted as treatment failure or true progression.

Part 3. Method for evaluating typical model parameters

Estimation of g. One way to estimate the tumor growth rate in a clinical setting is to assume that typical cancers are held in check, compared to more aggressive ones, at least partially by immune mechanisms, as suggested by clinical data on the emergence of tumors during immunosuppressive therapy for organ transplants(13, 37), as well as by the correlations of tumor associated lymphocyte numbers with clinical prognosis(14, 17, 27). In this case one can estimate the net growth rate, g, in the absence of immune mediated cell killing, from the doubling time of tumors of a given cell type in immunosuppressed patients. For minimally immunogenic tumors $dT/dt \approx gT$, or $dT/T \approx gdt$, from which, after integration, $T/T_0 \approx e^{gt}$. For doubling time t_2, in these selected patients it follows that $2 \approx e^{gt_2}$, or $g \approx \ln(2)/t_2 \approx 0.69/t_2$. For example, if tumors of a particular cell type in relatively immunosuppressed patients double in volume in 170 days after diagnosis, then we would have g = 0.004/day. This value is a starting point for our representative general model. It can be modified, as desired, for particular cancer types and patient populations going forward.

Estimation of k. For the equilibrium condition $dL/dt = 0$ we must have $k = g/L_0$. For example, if $g = 0.004$ /day, and $L_0 = 0.001$, then $k = 4$ tumor cells killed per lymphocyte per day. From considerations of practical biology a lymphocyte can only kill a handful of tumor cells per day(9). Hence values of $1 < k < 10$ are reasonable.

Estimation of L_0/T_0. Parameter L_0/T_0 can be obtained from biopsies of human tissue, as determined by quantitative microscopic analysis, flow cytometry, or histochemistry of excised tumors or biopsy specimens. Lymphocytes are microscopically detectable in many tumors(14, 17, 27). Previous simulations(3) suggest that values of L_0/T_0 can vary over many orders of magnitude and still result in successful tumor elimination by immunotherapy. Accordingly, this parameter is important to study over a wide range of values to represent the overall variability of cytokinetics during immunotherapy, especially in the setting of prior conventional chemotherapy.

Estimation of μ. Normal biology and clinical experience set limits on the value of lymphocyte decay, μ. The offset time for moderate to severe viral infections, which are combated by cellular immunity, is on the order of about one week. The exponential decay of the induration of a PPD (purified protein derivative) test for tuberculosis, mediated by cellular immunity, is also a few days to one or two weeks(38). Thus in the absence of stimulation ($\lambda LT = 0$) we would have $dL/dt = -\mu L$ or , $L/L_0 \approx e^{-\mu t}$. For half time $t_{1/2}$, it follows that $1/2 = e^{-\mu t_{1/2}}$, or $\mu = \ln(2)/t_{1/2} \approx 0.69/t_{1/2}$. For example, if the offset of a cellular immune response has a half-life of 7 days, then $\mu \approx 0.1$/day.

Estimation of λ. Using the relationship that at stalemate $\frac{dL}{dt} = \lambda L_0 T_0 - \mu L_0 = 0$, one can get a working estimate of $\lambda = \mu/T_0$. So, for $T_0 = 1$, representing the relative initial tumor population size as in Table 1, λ is estimated as 0.1/day. In this way reasonable mid-range approximations for parameters g, L_0/T_0, μ, and k, and λ can be determined from clinical data for particular types

of tumors. In the present Monte Carlo or stochastic models, individual cases were generated by randomly varying model parameters from the midrange values at stalemate listed in Table 1.

Table 1. Generic model parameters at stalemate with no net tumor growth, despite an active immune system

Parameter	Value and units	Description
T_0/T_0	1	Relative tumor cell count
L_0/T_0	0.001	Relative immune cell count
g	0.004/day	Tumor growth constant with minimal immune response
k	4/days	Immune cell killing effectiveness (tumor cells killed/lymphocyte/day)
λ	0.1/day/tumor cell	Immune cell signaling constant
μ	0.1/day	Spontaneous half-life decay of immunocytes

Part 4. Ranges of model parameters and statistical sampling

In the present problem there is a need to focus on clinically realistic ranges of parameters g, k, L_0/T_0, λ, and μ. An unrealistically wide range of parameter values, producing many obvious successes and many obvious failures would make simulated clinical decision making falsely easy. So, to determine if various possible decision making algorithms might be clinically useful, one needs to test difficult to distinguish cases. The studies presented here allowed variation of parameters over a range extending to twice the stalemate values in Table 1. Uniform probability distributions for parameters g, k, L_0/T_0, λ, and μ were used with upper and lower bounds shown in Table 2. To span the very large range of possible values of L_0/T_0, covering several orders of magnitude, sampling from a uniform distribution of the logarithm of L_0/T_0 was done.

Table 2. Lower and upper limits of model parameters in Monte Carlo simulations of difficult to distinguish cases

Parameter	Lower limit and units	Upper limit and units
g	0.001/day	0.009/day
k	0.1/day	10/day
$Log_{10}(L_0/T_0)$	-2	-8
λ	0.01 days/tumor cell	0.2 days/tumor cell
μ	0.01/day	0.2/day

Part 5. Tumor diameter changes at 2, 4, 6, 8, 10, and 12 months as predictors of success or failure

New guidelines(31) focus on changes in aggregate tumor diameter, d , vs. time as a marker for benefit vs. progression. Tumor diameter can be estimated at follow up by a variety of medical imaging methods. Diameter based measurements are highly precise and provide a standard metric for immune-related response(31). The present study uses the growth ratio d/d_0 as an easily computed mathematical surrogate for average nodule diameter. Here we can translate cell numbers into tumor size using the overall number of tumor cells, T, plus the overall number of lymphocytic cells, L in the tumor. This sum is assumed to be directly proportional to the tumor volume (average linear dimension cubed), and the relative diameter, d/d_0 , of tumor masses at follow up, so that d/d_0 is computed as $\sqrt[3]{(T+L)/(T_0+L_0)}$. Simulated data from full two-year (24 month) treatment histories are used to find the relationship between d/d_0 at 2, 4, 6, 8, 10, and 12 months and ultimate success or failure at 24 months.

Part 6. Histograms of diameter ratios for success and failure

To evaluate the effectiveness of d/d_0 as a predictor of success vs. failure, histograms are created for d/d_0 data at each bi-monthly follow up time during the first year, first for all successful treatments and then for all failed treatments. When the histograms show separation of the two populations on the d/d_0 axis, then one can set a decision threshold ("bar" or cutoff value) to predict failure early. If the tumor diameter ratio is less than an optimized cutoff value, then watchful waiting is in order and success is likely. However, if the tumor diameter ratio is greater than the optimized cutoff value, then failure is more likely, and the patient is better served by a change in treatment. The overall predictive value of this diagnostic test depends on the separation of the distributions of d/d_0 for successful and failed treatments.

Part 7. A raised bar for immunotherapy

The concept of "re-setting the bar" and for defining progressive disease has been advocated in the iRECIST guidelines for response criteria in trials testing immunotherapeutics(36). In the present context the bar can be time varying. As shown, for example, in Results Figure 6, the dashed vertical lines correspond to a particular d/d_0 cutoff levels at either 2, 4, 6, 8, 10, or 12 months. Optimization is done by trial and error and consideration of the value added by a simple and memorable rule-of-thumb.

RESULTS

Variable histories of immunotherapy

Figure 1 illustrates a variety of simulated histories of immunotherapy for the generic tumor model of Tables 1 and 2. Variations in tumor size are represented in terms of the tumor diameter ratio d/d_0 . The middle curve, labeled 1.0X, represents the unstable equilibrium model in Table 1. Other curves represent large or small deviations from the unstable equilibrium caused by the combined, reciprocal alteration of the two most influential model parameters, immune-tumor cell interaction, λ, and tumor growth rate, g. The monotonically increasing upper curve, labeled 0.2X, represents a poor outcome scenario in which immune response parameter, λ, is weakened by a factor of 0.2 and cell growth rate, g, is increased by a factor of 1/0.2 = 5.0. This curve describes ineffective treatment with runaway tumor growth. The monotonically decreasing lower curve, labeled 2.0X, represents a good outcome scenario, in which immune response parameter, λ, is strengthened by a factor of 2.0 and cell growth rate, g, is decreased by a factor of 1/2.0 = 0.5. This curve represents highly effective treatment. These clear-cut outcomes bracket a wide range of more complex dynamics.

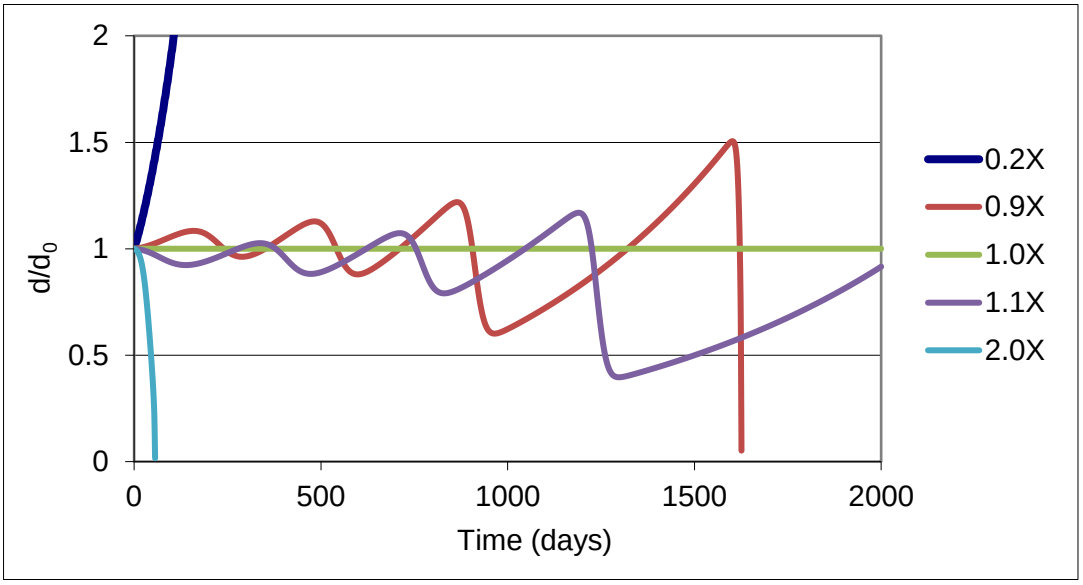

Figure 1. Simulated histories of tumor size in terms of diameter ratio, d/d_0 , after onset of immunotherapy. The middle curve, labeled 1.0X, represents the unstable equilibrium model in Table 1. Monotonically increasing upper curve, labeled 0.2X, represents a bad outcome, and monotonically decreasing bottom curve, labeled 2.0X, represents a rapid cure. Intermediate curves represent $\pm$10% changes in both tumor growth rate and immune signaling from the stalemate 1.0X condition.

The curve labeled 0.9X in Figure 1 represents only a slight weakening of immune response by 10 percent and a slight increase of tumor growth by 10 percent, compared to the stalemate conditions at 1.0X. This modest imbalance produces oscillatory behavior. There is an initial growth in tumor cell numbers, which then provokes an increased host response after a phase delay. This modest increase in host response in insufficient to destroy the tumor, however, and after a period of shrinkage, it starts to grow again. This cycle is repeated until a crescendo is reached after 1500 days or 50 months that finally provokes a sufficient immune response to destroy the tumor. The oscillation cycle time is about 1 year, and cure is delayed for 4 cycles.

Obversely, the curve labeled 1.1X represents only a slight strengthening of the immune response by 10 percent and a slight decrease of tumor growth by 10 percent. There is an initial decline in tumor cell numbers, which causes a subsequent decreased host response and allows for tumor regrowth. This cycle is repeated at 1-year intervals until a crescendo is reached after 4 years that eliminates the tumor. These simulations illustrate how very small changes in the balance of factors governing predator-prey dynamics can alter the time course and outcome of immunotherapy.

In Figure 2 the interplay of tumor cells and immune cells for two such closely matched battles is illustrated in terms of the relative tumor and immune cell numbers. T/T_0 is the ratio of the tumor cell count at the indicated time to the tumor cell count at time zero, and L/T_0 is the ratio of the lymphocyte count at the indicated time to the tumor cell count at time zero. In Figures 2(a) and 2(b) when $L_0/T_0 = 0.0008$ at time zero, the tumor can grow slightly, disturbing the equilibrium initially and provoking a further host response cyclically. After 1500 days the lymphocyte ratio gets just shy of the lethal level near 0.015, but a few tumor cells hang on. The tumor is not completely dead, but the lymphocytes go into hiding. This example represents a near cure.

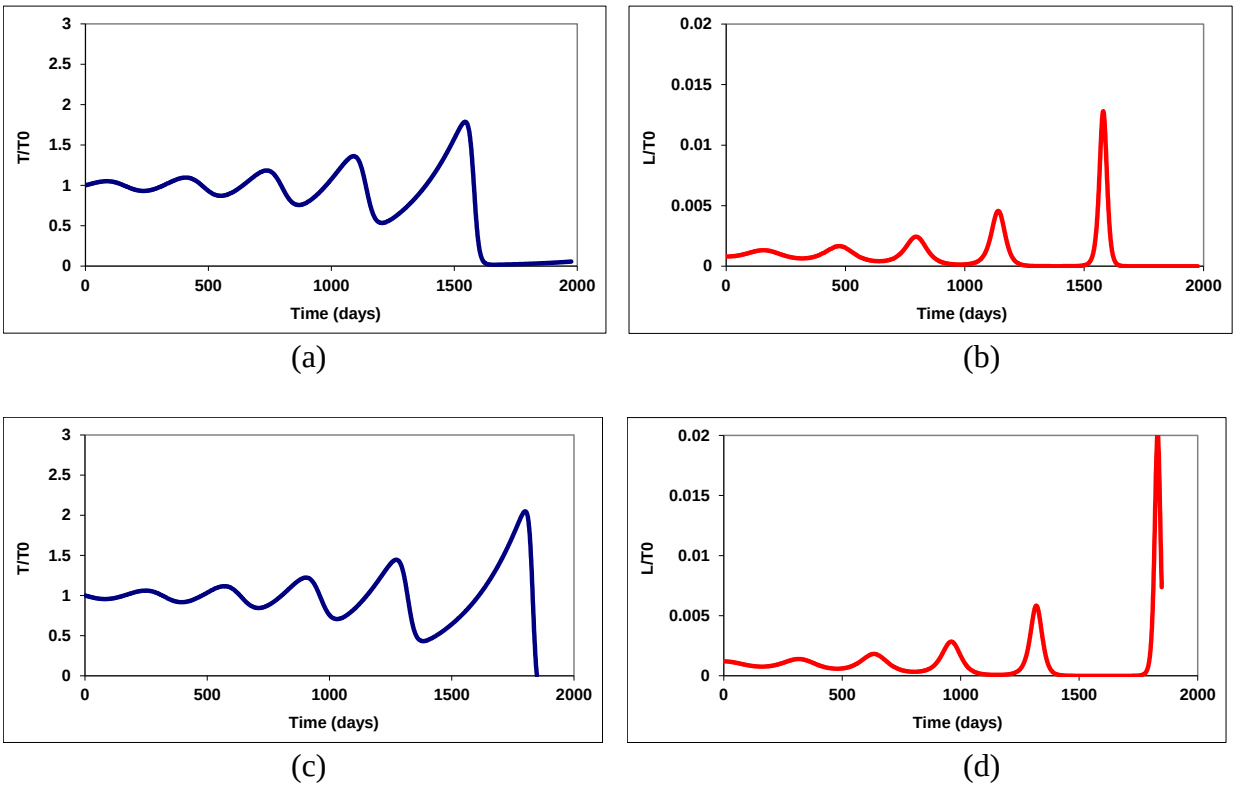

Figure 2. Histories of tumor and lymphocyte cell numbers, normalized by initial tumor cell count T0, for a representative prolonged, back-and-forth struggle between tumor cells and immunocytes. Growing oscillations in cell numbers occur with a cycle length of roughly 1 year and a phase delay of about 1/6 cycle or 2 months.

In Figures 2(c) and 2(d) $L_0/T_0 = 0.0012$, just slightly larger than the unstable stalemate equilibrium of 0.001 at time zero. The tumor shrinks slightly and there are oscillations around the equilibrium value of $T/T_0 = 1.0$. These non-intuitive results demonstrate sizeable oscillations with a period of 500 days in which the tumor mass grows to a maximum and then shrinks significantly. The immune response lags the tumor response in phase. In Figures 2(c) and 2(d) the oscillations gradually amplify until around 1800 days. Then the lymphocyte population finally grows beyond the threshold level near 0.015, which is sufficient to win the battle and kill the tumor completely.

Importance of the initial immune response

There are more anomalies, including the paradoxical result of success at very low $L_0/T_0 = 0.0000001$ (Figure 3). This value is several orders of magnitude less than the value 0.001 at steady state equilibrium. Now the tumor grows freely and quickly at first and doubles in size. Then it provokes a suprathreshold immune response that kills the last tumor cell at 264 days. Such dynamics are not generally seen with conventional anti-cancer chemotherapy.

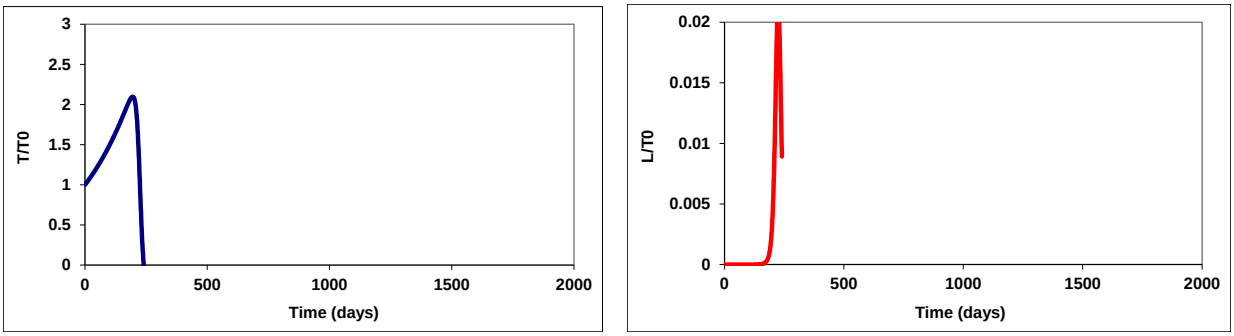

(a) (b)

Figure 3. Time histories of (a) tumor and (b) lymphocyte cell numbers in an extreme case of pseudoregression. Initial immune response is too weak to impact tumor growth, but after doubling of tumor cell mass the cell-cell signaling provokes a large and lethal immune response.

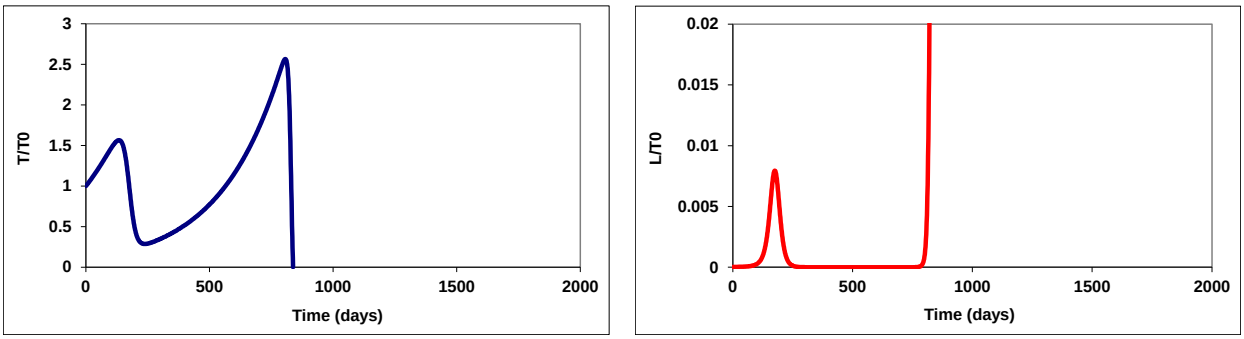

(a) (b)

Figure 4. Time histories of (a) tumor and (b) lymphocyte cell numbers in a rare case of partial response followed by extreme pseudoregression and ultimate tumor elimination after two years.

In Figure 4 with $L_0/T_0 = 0.00003$ (greater than the value in Figure 3) the initial tumor growth produces a strong response but not quite sufficient completely destroy the tumor. Regrowth happens until there is more than doubling of T_0, whereupon a lymphocyte population well over 1 in 100 tumor cells rises up to produce a complete cure, but only after 30 months of treatment. In this case the maximal diameter ratio, $d_{max}/d_0 \approx \sqrt[3]{2.5} \approx 1.34$.

In general, for a tumor model of a particular growth rate, g, success vs. failure is strongly influenced by differences in the initial immunocyte population size, L_0/T_0, over many orders of magnitude. Figure 5 shows the time course of tumor diameter for the otherwise standard model of Table 1 for each of several initial lymphocyte populations ranging over 8 orders of magnitude,

representing severely immunodeficient vs. strongly immunocompetent individuals. The models predict surprising and paradoxical responses that have also been observed in the clinic (see Discussion) and depend on particular kinetic interactions. The horizontal line labeled L0/T0 = 0.001 in Figure 5 indicates the stalemate condition of Table 1. If the initial immune response is either strengthened or weakened by one order of magnitude, oscillations over a 2 to 4 year time course happen, similar to those in Figure 2. However, if the initial lymphocyte population is reduced by 3 to 7 orders of magnitude, there is initial tumor diameter growth by about 1.3 to 1.5 fold, which is followed by rapid tumor cell killing and tumor elimination in less than 1 year.

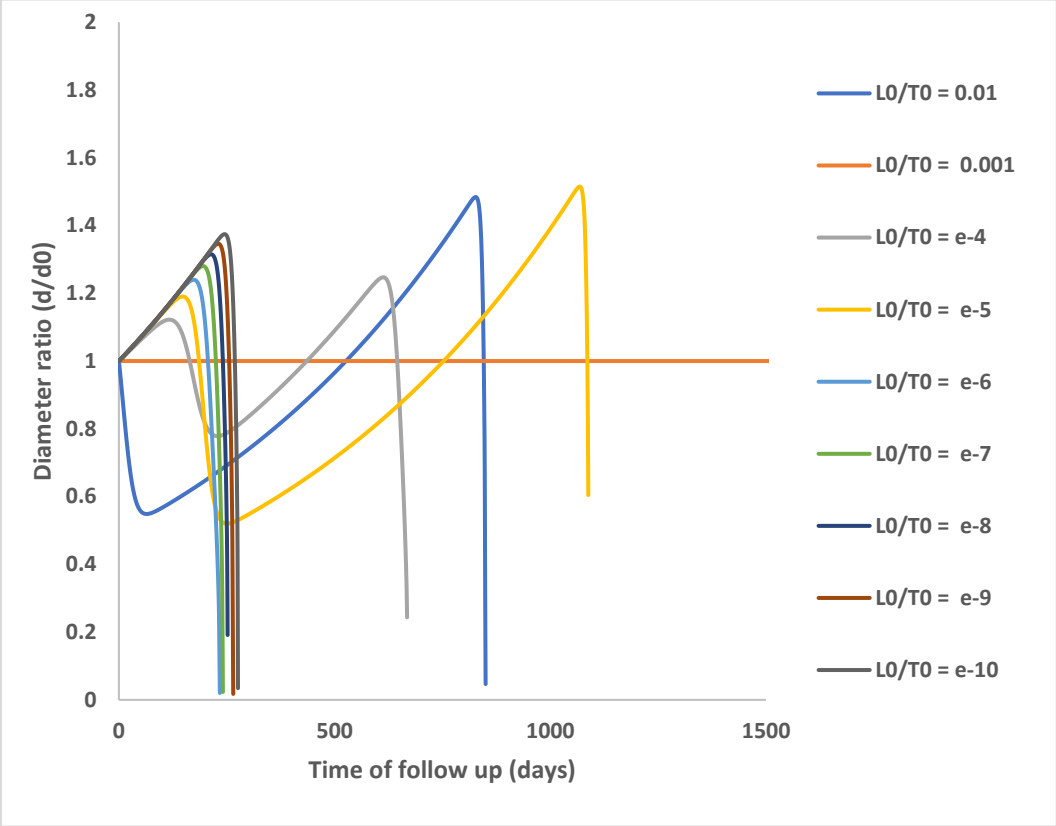

Figure 5. Simulated histories of tumor size after onset of immunotherapy for various values of L_0/T_0 , illustrating paradoxical effects of initial immune cell population size.

In the forgoing simulations, the tumor cells are constantly susceptible to cytotoxic cells with no development of resistance or tumor escape mechanisms. The exponential phases of growth are not related to tumor cell heterogeneity or evolution of resistant strains(12, 23), but to the underlying kinetics of predator-prey equations(5, 6). With fewer lymphocytes at time zero more tumor growth is needed to provoke an intense, and ultimately successful, anti-tumor immune response.

Histograms of successful vs. failed treatments

Figure 6 shows histograms of tumor diameter ratios for failed and successful courses of immunotherapy in a heterogeneous set of 4000 simulated patients having variations in model parameters, as shown in Table 2. The figures show the statistical distributions of d/d_0 values observed at either 2, 4, 6, 8, 10, or 12 months follow up along the horizontal axes and the corresponding probability density functions on the vertical axes. The probability density function (pdf) is scaled by sample size, such that the area under each pdf curve is exactly 1.00.

Circles represent d/d_0 values for failed treatments, according to the criteria listed previously. Squares represent d/d_0 values for successful treatments. At 2 months follow up, most cases show little change in diameter with d/d_0 near 1, except for a few treated cases with rapid shrinkage and d/d_0 near zero. At 4 and 6 months follow up, greater proportions of treated cases shrink toward zero diameter. At 8 and 12 months follow up, most successful cases show tumor regression, but a few remain near their original size or larger. At 8 and 12 months follow up, failed cases show a wide range of sizes, with some partially regressing and some cases continuing to grow. Importantly, in this particular model the distributions of successful and failed cases begin to separate as follow up continues. The completeness of the separation improves over time.

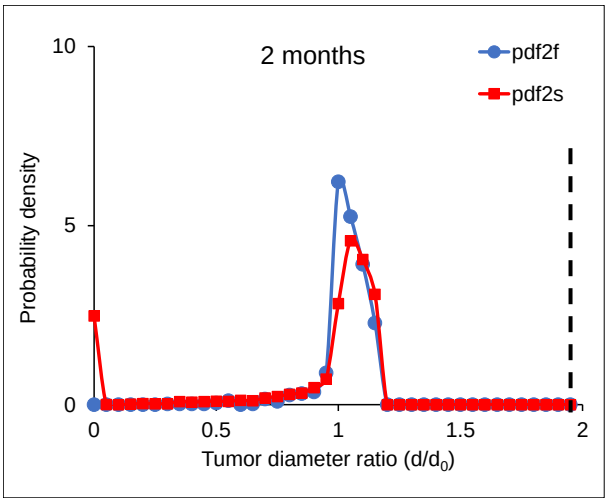
2 months
pdf2f
pdf2s
Probability density
Tumor diameter ratio (d/d0)

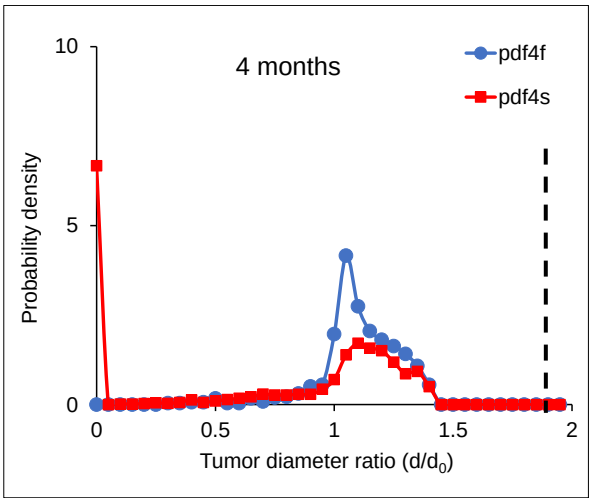
4 months
pdf4f
pdf4s
Probability density
Tumor diameter ratio (d/d0)

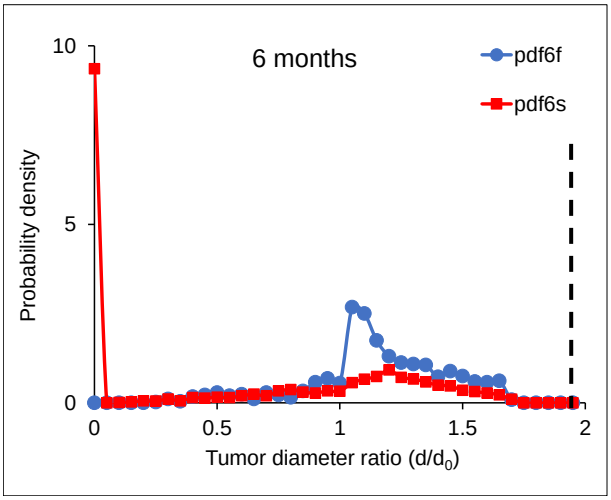
6 months
pdf6f
pdf6s
Probability density
Tumor diameter ratio (d/d0)

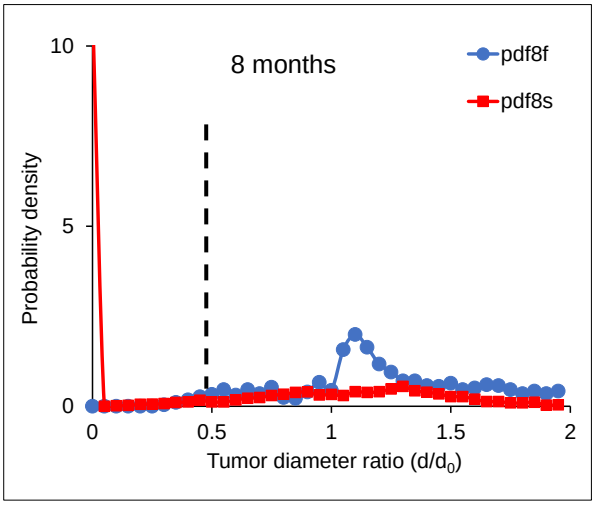
8 months
pdf8f
pdf8s
Probability density
Tumor diameter ratio (d/d0)

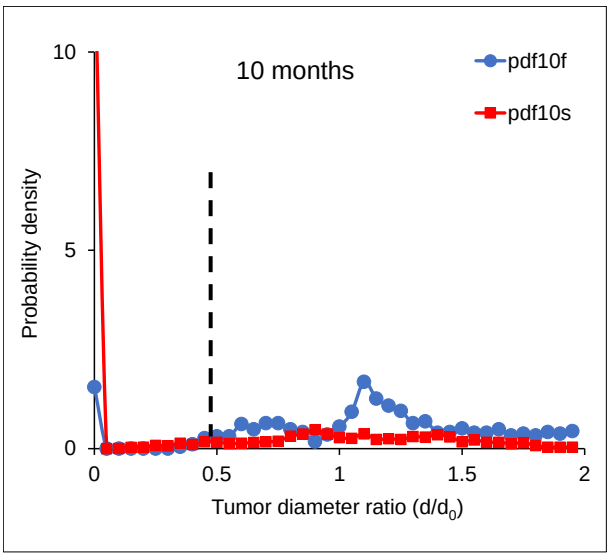
10 months
pdf10f
pdf10s
Probability density
Tumor diameter ratio (d/d0)

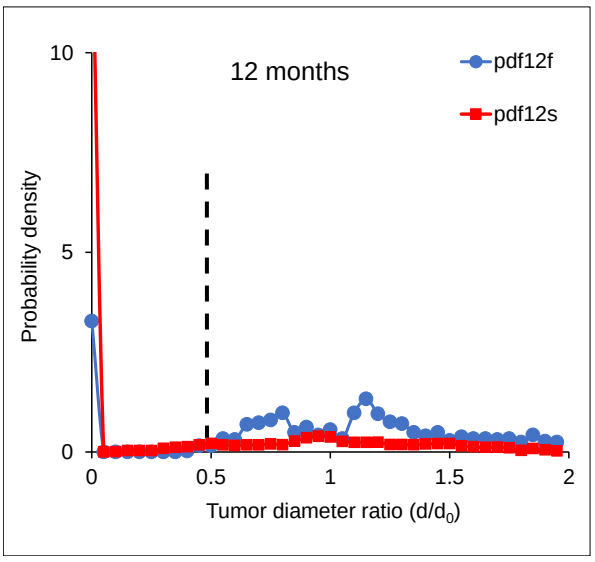
12 months
pdf12f
pdf12s
Probability density
Tumor diameter ratio (d/d0)

Figure 6. Histograms, scaled as probability density for easy comparison, of simulated successful and failed immunotherapy treatments based on predator-prey kinetic Equations (1) and (2). Square data points represent distributions of successful cases of tumor elimination within 2 years and circles represent distributions of failed cases of true progressive disease. Areas under the curves of all histograms are 1.00. Dashed lines represent decision thresholds for apparent progressive disease using a raised bar strategy, in which the bar is raised to 2.0 for the first 6 months of follow up and then lowered to 0.5.

The vertical dashed lines in Figure 6 represent a simple step-down protocol, in which a decision threshold of 2.0 is used for the first 6 months of follow up and then adjusted downward to 0.5 after 6 months. In the standard or reference protocol any increase in tumor diameter is considered as evidence of progression, with a constant decision threshold for progressive disease of $d/d_0 = 1.0$. The step-down paradigm eliminates many false alarms that could curtail ultimately successful therapy.

DISCUSSION

Compared to conventional chemotherapy, immunotherapy for cancer has very different kinetics that involve building an immune response (k and λ) from wide-ranging starting conditions. Several months are often required for an adequate T cell population explosion and for homing and infiltration of the tumor, after which there is therapeutic tumor cell killing. In clinical practice both physicians and patients, who are accustomed to the kinetics of conventional cancer chemotherapy, may be tempted to stop too soon. Better knowledge of immune response kinetics may allow better planning of clinical trials and better individual patient care to account for early, clinically insignificant progressive disease or "pseudoprogression"(7, 22, 33).

Mathematical models such as the one described here can help to explain the, complex, dynamical behavior of anti-tumor immunity(9, 24, 29, 43). The simplicity of Equations (1) and (2) encodes many emergent behaviors in the battle between immunocytes and cancer cells, including oscillations in tumor cell numbers, sharp thresholds between failed and completely successful therapy, improved success after weakening of anti-tumor response parameters, and initial tumor growth as a prelude to early tumor elimination. The variable histories of changes in tumor size simulated here (Figures 1 to 5) and previously(3), are similar to those observed in patients with malignant melanoma treated with anti-cytotoxic T lymphocyte-associated protein 4 immunotherapy (ipilimumab)(22). Present results suggest that growth or oscillations in tumor size after manipulation of the immune system need not imply selective resistance, escape mechanisms, or heterogeneity of the tumor cell population. Some initial tumor growth after treatment begins may simply reflect the nature of a predator-prey-like system. A very small initial population of lymphocytes can be sufficient to start a positive feedback cycle that ultimately results in tumor elimination, provided sufficient time is allowed for immune cell recruitment.

The kinetics of Equations (1) and (2) predict interesting apparent paradoxes that may explain treatment failures in early trials of immunotherapy. As shown previously by Babbs(3) and in Figure 1, a form of cyclic pseudoprogression can occur in which the tumor diameter alternately grows and shrinks for several cycles prior to a final stage of growth, which is followed by massive tumor cell kill. Such swings are an expected mathematical property of negative feedback control and not necessarily a sign of an incorrect hypothesis, sloppy technique, or human error. The rare cases in which tumor cell populations oscillate with increasing peak values are reminiscent of the phenomenon of concomitant tumor immunity mediated by a CD-8 T-cell response, in which challenge with a second tumor implant of the same type can stimulate immune rejection(16). Such unpredictability of dynamic interactions between immune response and tumor may mean that personalized patient specific strategies will be needed to achieve maximal success. Here computer simulations and models can help.

The concept of raising the bar for definition of progressive disease may provide practicing clinicians and their patients with useful guides to monthly management of immune therapy and the necessary encouragement to patiently wait for the immune treatment to work in its own characteristic way. Necessary data are tumor size vs. time curves from imaging studies that are already recommended for follow up in immunotherapy(22, 31). Aggregation of d/d_0 data from multiple imaging findings can reduce the average measurement error or "noise", which declines as a function of $1/\sqrt{n}$, where n is the number of tumor nodules measured. By monitoring tumor diameter growth versus time and using a raised threshold for defining progression during the first six months of follow up, one can accommodate expected initial growth in tumor size, as the lymphocytic response grows. This simple adjustment eliminates many false alarms signaling progressive disease, which in the setting of conventional chemotherapy would be of concern. Here a "raised bar" to 2.0 times original diameter (larger than the 1.2 threshold value recommended by Nishino et al.(31)) is shown to have a roughly optimal result on prediction accuracy, with little downside cost.

Limitations and future work

The present model includes only two differential equations and a handful of parameters. This is clearly an oversimplification. The complexity of immune mechanisms is well known(32). There are a host of T cell types, T cell exhaustion, pro-tumorigenic subsets of immune cells, checkpoints and checkpoint inhibitors, interactions with neutrophils and macrophages, and interactions with dendritic cells and myeloid-derived suppressor cells resulting in positive and negative feedback loops within the immune system, to name a few(7). Yet what is remarkable from the present study is how just two ordinary differential equations with lumped parameters can mimic the kinetics of immunotherapy of cancer to a reasonable degree--perhaps a rare case of the "less is more" principle.

Different initial levels of a raised bar may apply to different tumor types and stages. The present study focuses on one generic cancer type to illustrate proof of concept. However, the model and approach described here may well be applicable across a wide range of cancer types, as suggested by Seymour(36). Model parameters can be adjusted to fit different malignant diseases. Further, there is the added potential for tuning the parameters to make of the present

model patient specific. The value of g can be customized based on the patient's individual history. The value of L_0/T_0 can be customized based on individual biopsy results(10, 11, 28, 39). Perhaps in vitro tests could be done from biopsy material to estimate constants k and μ. Personalized values of λ might be estimated, based on specific biomarkers and adjusted for various immunotherapy combinations.

Here a general mathematical model is developed to describe the basic time-varying relationships of cancer, immunity, and immunotherapy. In the future patient specific parameters can be substituted for the general ones to create truly personalized models using Equations (1) and (2) in which the parameters are time-varying and adjusted to reflect changes in dosage, the use of adjuvants, or evolution of resistant tumor cell lines, combinations of conventional chemotherapy and immunotherapy(1, 8, 15), combinations of radiation and immunotherapy(18), as well as variability of cancer types and stages, prior treatments, and evolving mutations(40), conventional chemotherapy or radiation followed by immunotherapy(20, 41), targeted radiation to specific tumor masses that spares systemic damage to the patient's immune system, dose fractionation schemes, occasional drug holidays, etc. Adoptive immunotherapy(24, 30, 34), for example, can be simulated by a boost in L_0. Adjunctive treatment with immune modifiers such as imiquimod(35) can be represented by a boost in λ. Another strategy to increase λ might be to reduce the level of suppressive cells (T_{reg} and myeloid-derived suppressor cells) (1). Supplemental radiation treatment can be represented approximately by temporarily replacing the positive growth constant, g, with a negative value, so that each cell cycle would then lead to death rather than replication. Many such scenarios are open to investigation. The present model might help to predict especially promising ones for future laboratory or clinical testing.

DISCLOSURE OF INTEREST

The author reports no conflict of interest.

FUNDING DETAILS

This work was supported by Purdue University internal funds.

REFERENCES

1. **Abastado JP**. The next challenge in cancer immunotherapy: controlling T-cell traffic to the tumor. *Cancer research* 72: 2159-2161, 2012.
2. **Agur Z, Halevi-Tobias K, Kogan Y, and Shlagman O**. Employing dynamical computational models for personalizing cancer immunotherapy. *Expert Opin Biol Ther* 16: 1373-1385, 2016.
3. **Babbs CF**. Predicting success or failure of immunotherapy for cancer: insights from a clinically applicable mathematical model. *Am J Cancer Res* 2: 204-213, 2012.
4. **Balwit JM, Hwu P, Urba WJ, and Marincola FM**. The iSBTc/SITC primer on tumor immunology and biological therapy of cancer: a summary of the 2010 program. *J Transl Med* 9: 18, 2011.
5. **Bell G**. Predator-prey equations simulating an immune response. *Mathematical Biosciences* 16: 291-314, 1973.
6. **Berryman AA**. The origins and evolution of predator-prey theory. *Ecology* 73: 1530-1535, 1992.
7. **Champiat S, Ferrara R, Massard C, Besse B, Marabelle A, Soria JC, and Ferte C**. Hyperprogressive disease: recognizing a novel pattern to improve patient management. *Nat Rev Clin Oncol* 15: 748-762, 2018.
8. **Copier J, Dalgleish AG, Britten CM, Finke LH, Gaudernack G, Gnjatic S, Kallen K, Kiessling R, Schuessler-Lenz M, Singh H, Talmadge J, Zwierzina H, and Hakansson L**. Improving the efficacy of cancer immunotherapy. *Eur J Cancer* 45: 1424-1431, 2009.
9. **De Boer RJ, Hogeweg P, Dullens HF, De Weger RA, and Den Otter W**. Macrophage T lymphocyte interactions in the anti-tumor immune response: a mathematical model. *J Immunol* 134: 2748-2758, 1985.
10. **Denkert C, Loibl S, Noske A, Roller M, Muller BM, Komor M, Budczies J, Darb-Esfahani S, Kronenwett R, Hanusch C, von Torne C, Weichert W, Engels K, Solbach C, Schrader I, Dietel M, and von Minckwitz G**. Tumor-associated lymphocytes as an independent predictor of response to neoadjuvant chemotherapy in breast cancer. *J Clin Oncol* 28: 105-113, 2010.
11. **Djenidi F, Adam J, Goubar A, Durgeau A, Meurice G, de Montpreville V, Validire P, Besse B, and Mami-Chouaib F**. CD8+CD103+ tumor-infiltrating lymphocytes are tumor-specific tissue-resident memory T cells and a prognostic factor for survival in lung cancer patients. *J Immunol* 194: 3475-3486, 2015.
12. **Drake CG, Jaffee E, and Pardoll DM**. Mechanisms of immune evasion by tumors. *Advances in immunology* 90: 51-81, 2006.
13. **Euvrard S, Kanitakis J, and Claudy A**. Skin cancers after organ transplantation. *The New England journal of medicine* 348: 1681-1691, 2003.
14. **Galon J, Costes A, Sanchez-Cabo F, Kirilovsky A, Mlecnik B, Lagorce-Pages C, Tosolini M, Camus M, Berger A, Wind P, Zinzindohoue F, Bruneval P, Cugnenc PH, Trajanoski Z, Fridman WH, and Pages F**. Type, density, and location of immune cells within human colorectal tumors predict clinical outcome. *Science (New York, NY* 313: 1960-1964, 2006.
15. **Gatenby RA**. Application of competition theory to tumour growth: implications for tumour biology and treatment. *Eur J Cancer* 32A: 722-726, 1996.

16. **Gershon RK, Carter RL, and Kondo K**. On concomitant immunity in tumour-bearing hamsters. *Nature* 213: 674-676, 1967.
17. **Gooden MJ, de Bock GH, Leffers N, Daemen T, and Nijman HW**. The prognostic influence of tumour-infiltrating lymphocytes in cancer: a systematic review with meta-analysis. *British journal of cancer* 105: 93-103.
18. **Gough M, Sharon S, Crittenden M, and Young K**. Using Preclinical Data to Design Combination Clinical Trials of Radiation Therapy and Immunotherapy. *Semin Radiat Oncol* 30: 158-172, 2019.
19. **Hanahan D, and Weinberg RA**. Hallmarks of cancer: the next generation. *Cell* 144: 646-674, 2011.
20. **Harris TJ, Hipkiss EL, Borzillary S, Wada S, Grosso JF, Yen HR, Getnet D, Bruno TC, Goldberg MV, Pardoll DM, DeWeese TL, and Drake CG**. Radiotherapy augments the immune response to prostate cancer in a time-dependent manner. *The Prostate* 68: 1319-1329, 2008.
21. **Hoos A, and Britten C**. The immuno-oncology framework: Enabling a new era of cancer therapy. *Oncoimmunology* 1: 334-339, 2012.
22. **Hoos A, Eggermont AM, Janetzki S, Hodi FS, Ibrahim R, Anderson A, Humphrey R, Blumenstein B, Old L, and Wolchok J**. Improved endpoints for cancer immunotherapy trials. *J Natl Cancer Inst* 102: 1388-1397, 2010.
23. **Kirkwood JM, Tarhini AA, Panelli MC, Moschos SJ, Zarour HM, Butterfield LH, and Gogas HJ**. Next generation of immunotherapy for melanoma. *J Clin Oncol* 26: 3445-3455, 2008.
24. **Kirschner D, and Panetta JC**. Modeling immunotherapy of the tumor-immune interaction. *Journal of mathematical biology* 37: 235-252, 1998.
25. **Kronik N, Kogan Y, Elishmereni M, Halevi-Tobias K, Vuk-Pavlovic S, and Agur Z**. Predicting outcomes of prostate cancer immunotherapy by personalized mathematical models. *PLoS One* 5: e15482, 2010.
26. **Kronik N, Kogan Y, Vainstein V, and Agur Z**. Improving alloreactive CTL immunotherapy for malignant gliomas using a simulation model of their interactive dynamics. *Cancer Immunol Immunother* 57: 425-439, 2008.
27. **Leffers N, Gooden MJ, de Jong RA, Hoogeboom BN, ten Hoor KA, Hollema H, Boezen HM, van der Zee AG, Daemen T, and Nijman HW**. Prognostic significance of tumor-infiltrating T-lymphocytes in primary and metastatic lesions of advanced stage ovarian cancer. *Cancer Immunol Immunother* 58: 449-459, 2009.
28. **Mansuri N, Birkman EM, Heuser VD, Lintunen M, Algars A, Sundstrom J, Ristamaki R, Lehtinen L, and Carpen O**. Association of tumor-infiltrating T lymphocytes with intestinal-type gastric cancer molecular subtypes and outcome. *Virchows Arch* 478: 707-717, 2021.
29. **Mohler RR, Asachenkov AL, and Marchuk GI**. A systems approach to immunology and cancer. *IEEE Transactions on Systems, Man, and Cybernetics* 24: 632-642, 1994.
30. **Morgan RA, Dudley ME, Wunderlich JR, Hughes MS, Yang JC, Sherry RM, Royal RE, Topalian SL, Kammula US, Restifo NP, Zheng Z, Nahvi A, de Vries CR, Rogers-Freezer LJ, Mavroukakis SA, and Rosenberg SA**. Cancer regression in patients after transfer of genetically engineered lymphocytes. *Science (New York, NY* 314: 126-129, 2006.

31. **Nishino M, Giobbie-Hurder A, Gargano M, Suda M, Ramaiya NH, and Hodi FS**. Developing a common language for tumor response to immunotherapy: immune-related response criteria using unidimensional measurements. *Clin Cancer Res* 19: 3936-3943, 2013.
32. **Pardoll D**. Cancer and the Immune System: Basic Concepts and Targets for Intervention. *Seminars in oncology* 42: 523-538, 2015.
33. **Ribas A, Chmielowski B, and Glaspy JA**. Do we need a different set of response assessment criteria for tumor immunotherapy? *Clin Cancer Res* 15: 7116-7118, 2009.
34. **Robbins PF, Morgan RA, Feldman SA, Yang JC, Sherry RM, Dudley ME, Wunderlich JR, Nahvi AV, Helman LJ, Mackall CL, Kammula US, Hughes MS, Restifo NP, Raffeld M, Lee CC, Levy CL, Li YF, El-Gamil M, Schwarz SL, Laurencot C, and Rosenberg SA**. Tumor regression in patients with metastatic synovial cell sarcoma and melanoma using genetically engineered lymphocytes reactive with NY-ESO-1. *J Clin Oncol* 29: 917-924.
35. **Ryu J, and Yang FC**. A review of topical imiquimod in the management of basal cell carcinoma, actinic keratoses, and other skin lesions. *Clinical Medicine: Therapeutics* 1: 1557-1575, 2009.
36. **Seymour L, Bogaerts J, Perrone A, Ford R, Schwartz LH, Mandrekar S, Lin NU, Litiere S, Dancey J, Chen A, Hodi FS, Therasse P, Hoekstra OS, Shankar LK, Wolchok JD, Ballinger M, Caramella C, de Vries EGE, and group Rw**. iRECIST: guidelines for response criteria for use in trials testing immunotherapeutics. *Lancet Oncol* 18: e143-e152, 2017.
37. **Starzi TE, Porter KA, Iwatsuki S, Rosenthal JT, Shaw BW, Atchison RW, Nalesnik MA, Ho M, Griffith BP, Hakala TR, Hardesty RL, Jaffee R, and Bahnson HT**. Reversibility of lymphomas and lymphoproliferative lesions developing under cyclosporin-steroid therapy *The Lancet* 322: 583-587, 1984.
38. **Tat D, Polenakovik H, and Herchline T**. Comparing interferon- gamma release assay with tuberculin skin test readings at 48-72 hours and 144-168 hours with use of 2 commercial reagents. *Clin Infect Dis* 40: 246-250, 2005.
39. **Tokito T, Azuma K, Kawahara A, Ishii H, Yamada K, Matsuo N, Kinoshita T, Mizukami N, Ono H, Kage M, and Hoshino T**. Predictive relevance of PD-L1 expression combined with CD8+ TIL density in stage III non-small cell lung cancer patients receiving concurrent chemoradiotherapy. *Eur J Cancer* 55: 7-14, 2016.
40. **Ventola CL**. Cancer Immunotherapy, Part 3: Challenges and Future Trends. *P T* 42: 514-521, 2017.
41. **Wada S, Yoshimura K, Hipkiss EL, Harris TJ, Yen HR, Goldberg MV, Grosso JF, Getnet D, Demarzo AM, Netto GJ, Anders R, Pardoll DM, and Drake CG**. Cyclophosphamide augments antitumor immunity: studies in an autochthonous prostate cancer model. *Cancer research* 69: 4309-4318, 2009.
42. **Wolchok JD, Hoos A, O'Day S, Weber JS, Hamid O, Lebbe C, Maio M, Binder M, Bohnsack O, Nichol G, Humphrey R, and Hodi FS**. Guidelines for the evaluation of immune therapy activity in solid tumors: immune-related response criteria. *Clin Cancer Res* 15: 7412-7420, 2009.
43. **Zhivkov P, and Waniewski J**. Modelling tumour-immunity interactions with different simulation functions. *Int J Appl Math Comput Sci* 13: 307-315, 2003.